ELSEVIER

Ocean Modelling 4 (2002) 313–325

Ocean Modelling

www.elsevier.com/locate/omodol

Sensitivity of numerical tracer trajectories to uncertainties in OGCM velocity fields

D. Iudicone [a,*], G. Lacorata [b,c], V. Rupolo [d], R. Santoleri [a], A. Vulpiani [e,f]

[a] *IFA-CNR, Area di ricerca di Tor Vergata, via Fosso del Cavaliere 100, I-00133 Roma, Italy*
[b] *Dipartimento di Fisica, Università dell'Aquila, via Vetoio 1, I-67010 Coppito, L'Aquila, Italy*
[c] *Dipartimento di Fisica, Università di Roma "La Sapienza", Piazzale Aldo Moro 5, I-00185 Roma, Italy*
[d] *Casaccia, ENEA, via Anguillarese 301, I-00060 Roma, Italy*
[e] *Istituto Nazionale Fisica della Materia, Unità di Roma 1, Roma, Italy*
[f] *Dipartimento di Fisica, Università di Roma "La Sapienza", Piazzale Aldo Moro 5, I-00185 Roma, Italy*

Abstract

Three different data sets of numerical drifters are obtained with degrading the time sampling (1 day, 1 month and 1 year) of the Eulerian velocity field computed from a Mediterranean general circulation model. The Finite-Scale Lyapunov Exponent (FSLE) technique is used to characterize, for each of the three data sets, Lagrangian dispersion properties in relation to the time resolution of the field. In particular, we are interested in measuring the unpredictability of trajectories due to the uncertainty in the knowledge of the velocity field. Our data analysis indicates that surface relative dispersion of the Mediterranean Sea has two regimes: exponential spreading due to chaotic advection at small scales (~mesoscale) and super-diffusion at larger scales (up to ~sub-basin scales). In this scenario, it is shown that trajectory evolution is most sensitive to the time sampling of the field at small spatial scales, while, at scales larger than ~100 km, it is essentially independent from the details of the models. Also, FSLE is employed to visualize the geographical regions characterized by high Lagrangian unpredictability. The relation of FSLE with common oceanographic observables (e.g., local shear, velocity variance) is discussed. © 2002 Published by Elsevier Science Ltd.

1. Introduction

Chaotic advection is the basic mechanism for Lagrangian transport and mixing in 3-D steady or time dependent velocity fields. It is well known that even regular (e.g. laminar and periodic in

* Corresponding author.
E-mail address: danele@lagrange.ifa.rm.cnr.it (D. Iudicone).

1463-5003/02/$ - see front matter © 2002 Published by Elsevier Science Ltd.
PII: S1463-5003(02)00006-9

time) Eulerian fields can determine a very complex and unpredictable Lagrangian behavior, mixing of particles and fine spatial scale structure of tracer distribution (Ottino, 1989). Under conditions of Lagrangian chaos, the study of the effects of uncertainties in the evolution law of trajectories (e.g. due to the coarse-graining of the velocity field), the so-called predictability problem of second kind (Lorenz, 1996), is a delicate issue. Some numerical experiments on dynamical systems, e.g., the Gollub model for Rayleigh-Bènard convection or shell models for 3-D turbulence (Boffetta et al., 2000a), show that transport properties at small spatial scales are strongly affected by the details of the evolution equations, whereas at large scales the transport properties become less sensitive to the uncertainty in the knowledge of the Eulerian fields.

Lagrangian numerical trajectories are used to extract, for instance, relevant physical information from the huge amount of data normally produced by Ocean General Circulation Models (OGCMs) (Blanke et al., 1999), but model simulations are expensive, especially when a Lagrangian integration scheme is added to the code. The result is that often asymptotic limits in the dispersion regimes cannot be achieved (Joseph and Swathi, 1999). On the other hand, Lagrangian computations can be done more efficiently *off-line*, i.e. using model-generated velocity fields, and in this case a relevant problem is the choice of the time sampling of the model output. Previous studies on Lagrangian transport in ocean models have proposed opposite strategies to overcome this inconvenient that consist in increasing the computational effort on the time resolution at the expense of decreasing the numbers of trajectories (Haines et al., 1999), or vice versa, (Döös, 1995).

We introduce here a technique that can be used to quantitatively estimate, for different spatial scales, the uncertainty on the Lagrangian evolution due to the time resolution of the Eulerian

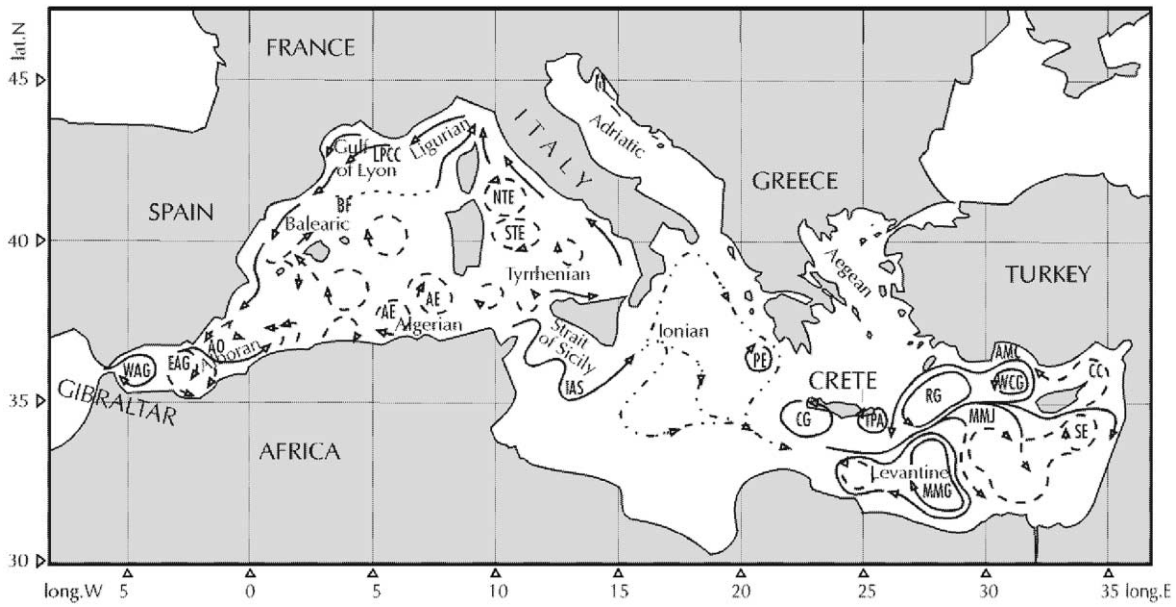

Fig. 1. Surface circulation of the Mediterranean sea.

velocity field. The classical approach to dispersion and mixing involves asymptotic quantities (long times, large scales) whereas geophysical systems are generally not suitable to this kind of standard analysis because of the presence of boundaries (Artale et al., 1997). Moreover, other complications arise in presence of regions of the domain that are non-stationary from a Lagrangian point of view (Figueroa and Olson, 1994). In this work, we study the surface (horizontal) dispersion of numerical drifters advected by velocity fields generated by an OGCM. We adopt the Finite Scale Lyapunov Exponent (FSLE) technique (Boffetta et al., 2000b) to characterize finite-scale dispersion and to estimate the effects of finite-time resolution of the velocity field on the off-line Lagrangian integrations.

We will analyze output data of an OGCM describing the Mediterranean Sea, where topographic and domain boundaries constraints strongly influence the circulation. The surface circulation (Fig. 1) can be characterized, in terms of spatial scales, as consisting of the mesoscale ($\sim$10 km), the gyre or sub-basin scale (100–300 km) and the basin scale circulation (up to a few thousands of km) (see Millot (1999), and POEM Group (1992) for the acronyms).

In such a basin, where Eulerian coherent structures reach the basin scale and Lagrangian transport is strongly affected by the domain boundaries, the classical approach to diffusion fails and more appropriate tools are needed. The aim of this paper is to present a new methodology (the FSLE); in a forthcoming paper, we will discuss in more detail the oceanographic implications of the outcome of this kind of analysis.

2. Predictability analysis

In this section, we briefly recall the concept of FSLE as estimator of relative dispersion. More details can be found in Boffetta et al. (2000b). Let us denote l_0 the smallest characteristic length and L_0 the largest characteristic length (e.g., the big gyre size) of a velocity field. If $\mathbf{x}^{(1)}$ and $\mathbf{x}^{(2)}$ are the position vectors of two particles, the (horizontal) relative dispersion is defined as

$$\langle R^2(t)\rangle = \langle \|\mathbf{x}^{(1)}(t) - \mathbf{x}^{(2)}(t)\|^2\rangle, \tag{1}$$

where the average is performed over a large number of trajectory pairs. The norm in (1) is the length of the great circle arc connecting two particle positions. Since we consider only particles within the surface layer, we neglect the vertical relative displacement. The quantity in (1) generally grows driven by Lagrangian chaos at very small scales ($\ll l_0$), and by diffusion at very large scales ($\gg L_0$). Lagrangian Maximum Lyapunov Exponent (MLE)

$$\lambda = \lim_{t\to\infty} \lim_{R(0)\to 0} \frac{1}{t} \ln \frac{R(t)}{R(0)} \tag{2}$$

measures the typical exponential growth rate of the distance $R(t)$ between two trajectories arbitrarily close at the initial time, i.e. as long as $R(t)$ remains *infinitesimal*. It is very difficult to compute λ in realistic situations, where the finite resolution prevents the knowledge of the small spatial scale components. In addition, when the interest is focused on the large scale properties, MLE is of questionable relevance.

On the other hand, effective diffusion coefficient

$$D = \lim_{t\to\infty} \frac{1}{4t}\langle R^2(t)\rangle \tag{3}$$

requires asymptotic conditions to be defined, i.e. long times and large scales, while over finite times, $\langle R^2(t)\rangle$ can lead to inconclusive or misleading behaviors (see also Artale et al., 1997). In terms of one-particle diffusion, the first zero-crossing of the Lagrangian velocity correlation is not observable when the advective time is of the same order or less than the Lagrangian decorrelation time (Figueroa and Olson, 1994). In this case, a two-particle statistics can be adopted to characterize the effective relative dispersion using the FSLE as a non-asymptotic measure of the relative dispersion rate (Boffetta et al., 2000b). The FSLE is defined as

$$\lambda(\delta, r) = \frac{1}{\langle \tau_r(\delta)\rangle} \ln r, \tag{4}$$

where δ is the size of the initial perturbation (here δ indicates the finite size relative distance between two trajectories) and $\langle \tau_r(\delta)\rangle$ is the mean time needed to amplify δ of a factor $r > 1$, averaged over a large number of realizations. In other words, $\lambda(\delta, r)$ measures how rapidly the initial distance δ grow to $r \cdot \delta$, within a range of non-infinitesimal scales, and does not depend much (or at all) on r if r is close to 1. A typical value is $r = \sqrt{2}$, which will be used henceforth, unless otherwise stated.

The FSLE is suitable to describe the dispersion between particles at finite scales (up to sub-basin scales) in non-asymptotic conditions, i.e., when the diffusive regime is not yet clearly established (see also Lacasce and Bower (2000) for an oceanographic application). The behavior of the FSLE in two limiting cases is well known: for infinitesimal δ, we have $\lambda(\delta) = \lambda$; in the large scale limit, in presence of a diffusion regime scaling $\langle R^2(t)\rangle \sim t^{\alpha}$, we have the correspondent scaling $\lambda(\delta) \sim \delta^{-2/\alpha}$. In the standard diffusion regime (i.e., $\alpha = 1$) one has $\lambda(\delta) \sim D \cdot \delta^{-2}$, as can be verified with a dimensional argument. It is worth noting that the quantity $\lambda(\delta)$ can also measure the predictability of a trajectory under perturbation of the evolution equations (Boffetta et al., 2000a). We shall call $\lambda_{\mathrm{I}}(\delta)$ and $\lambda_{\mathrm{II}}(\delta)$ the first kind and the second kind FSLE, respectively. The first kind FSLE is the one defined in Eq. (4). The second kind FSLE is introduced to study the second kind predictability. In this case, δ is the distance between the *true* trajectory, computed using the most detailed velocity field, and the *model* trajectory, computed with some approximate evolution equations, e.g., obtained with degrading the time sampling of the Eulerian velocity field. The trajectories start from the same point but are advected by different velocity fields. The exponents $\lambda_{\mathrm{I}}(\delta)$ and $\lambda_{\mathrm{II}}(\delta)$ generally overlap for $\delta > \delta^*$, where δ^* (if exists) is the threshold above which the uncertainty of the *model* relatively to the *true* system has no more influence. In the other limit, when the differences in trajectory evolution are dominant the two exponents tend to diverge from one another as δ^{-1} for $\delta \to 0$ (Boffetta et al., 2000a).

3. Trajectory computation

The OGCM is the Geophysical Fluid Dynamical Laboratory Modular Ocean Model (GFDL-MOM), adapted to the Mediterranean basin with the horizontal resolution of a 0.25° and 19 vertical levels (see Artale et al. (2002) for details). The model configuration is the same as de-

scribed in Roussenov et al. (1995) with some refinements in the parameterization of the tracer diffusivity and of the relaxation time to the surface temperature field. Surface temperature and salinity are relaxed to the 1988 NASA Pathfinder daily satellite sea surface temperature and the monthly surface salinity obtained from climatological data set. The daily wind stress is computed from ECMWF 1988 surface wind data. The simulated velocity patterns represent well the main Mediterranean current systems. As a test on its reliability, the model surface Eddy Kinetic Energy (EKE) has been compared with an estimate of EKE derived from TOPEX/Poseidon (T/P) altimeter data. Basinwide averages were found to be similar and a good agreement was found for the spatial distribution and local values of variability.

Lagrangian particles are integrated using the velocity field obtained from the 100th year of integration that is representative of the steady-state reached by the model. Three different experiments are performed using a time-independent yearly averaged (Y), and two periodic monthly (M) and daily (D) averaged velocity fields. In the following, we will study the effect of the uncertainities in the evolution law of trajectories considering as the *true* system the Lagrangian data set obtained sampling the Eulerian velocity field at the highest rate (D) and as the *perturbed* or *model* systems the other two other dat sets (M and Y) obtained with a coarse sampling of the Eulerain velocity field. A detailed description of the particle integration algorithm can be found in Blanke et al. (1999). Time dependence is introduced in this off-line integration algorithm by assuming that the Eulerian velocity is constant over periods shorter than or equal to the chosen sampling interval. For each grid point two pairs of particles, with a relative displacement of about 5 km, are simultaneously released at 80 m depth, for a total number of 7250 trajectory pairs. In order to consider only surface circulation inside the Mediterranean basin, the trajectory computation is stopped either when the particle reaches 200 m of depth, a representative lower limit for the surface layer in most of the basin, or exits through the Gibraltar strait. Trajectories are stored at a rate of one point per day.

4. Results

4.1. First kind analysis

First, relative dispersion was computed for each data set (D, M and Y; Fig. 2). The standard diffusion regime (slope = 1/2) is not yet visible at time delay of some years, when saturation effects set in. The overall growth of the mean distance between particles in time is consistent with a ballistic-like dispersion, i.e., with a non-zero mean relative velocity between particles (see below). In the D and M cases, the dispersion curves are quite similar while in the Y case the particle spreading is underestimated, indicating non-negligible time variabilities in the velocity field.

Let us define $\lambda_{\mathrm{I}}^{(\mathrm{D})}(\delta)$, $\lambda_{\mathrm{I}}^{(\mathrm{M})}(\delta)$ and $\lambda_{\mathrm{I}}^{(\mathrm{Y})}(\delta)$ as the first kind FSLE for the D, M and Y cases, respectively, computed over 7250 trajectory pairs. In Fig. 3 (upper and intermediate panel), we can see that $\lambda_{\mathrm{I}}^{(\mathrm{D})}(\delta)$ and $\lambda_{\mathrm{I}}^{(\mathrm{M})}(\delta)$ are very similar.

The plateau at small scales (up to about 60–70 km) indicates chaotic advection with a Lyapunov exponent $\sim 0.02\ \mathrm{day}^{-1}$, corresponding to a characteristic time equal to a few months. For larger spatial scales a negative slope is observed up to about 700 km where a change in behavior appears at the scale of sub-basin main circulation. The value for the slope at intermediate

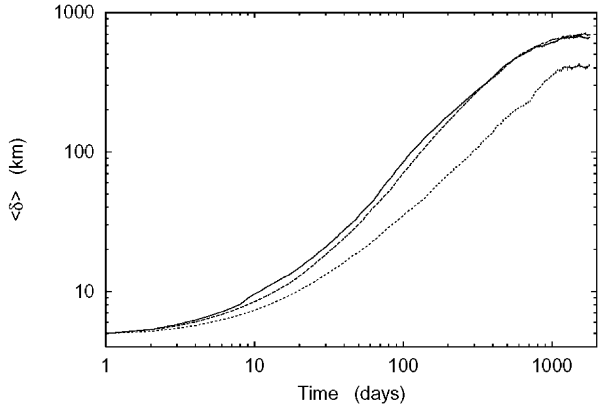

Fig. 2. Relative dispersion averaged over 7250 particle pairs advected with the three velocity fields: D, M and Y (upper, middle and lower curve, respectively).

scales is close to -1 and it is then compatible with a ballistic-like (or shear) dispersion, likely due to the persistence of a non-zero mean relative velocity when the two particles move along separated current systems. On the other hand, $\lambda_{\mathrm{I}}^{(\mathrm{Y})}(\delta)$ (Fig. 3, lower panel) clearly describes a model with lower dispersion properties. The plateau at small spatial scales is about one third of the value relative to the D and M cases and the curve bend is at about 350 km, i.e., at the scales of main gyres (recirculations). At basin scales, the FSLE begins to flatten probably due to saturation effects. The annual averaging filters out the mesoscale component and the dispersion properties are mainly determined by gyres and strong currents (e.g., Algerian current).

4.2. Second kind analysis

Following the terminology introduced in Section 2, we assume as the *true* system the D case, and as the *model* systems the M and Y cases and we compute the growth rate of the distance between trajectories starting from the same point but advected in the different systems. Here the uncertainty source is due to the different updating frequency of the velocity field within one year. The data sets are the same described above (7250 particle pairs) but the pairs now are formed with parcels from different data sets. The initial distance in this case is zero, and we start to compute the second kind FSLE when the threshold $\delta_1 = 5$ km is reached. We shall call $\lambda_{\mathrm{II}}^{(\mathrm{MD})}(\delta)$ and $\lambda_{\mathrm{II}}^{(\mathrm{YD})}(\delta)$, respectively, the second kind FSLE of M and Y (the model systems) relatively to (the true system) D. We report $\lambda_{\mathrm{II}}^{(\mathrm{MD})}(\delta)$ and $\lambda_{\mathrm{II}}^{(\mathrm{YD})}(\delta)$ in Fig. 4, with superimposed the graph of the mean values of $\lambda_{\mathrm{I}}^{(\mathrm{D})}(\delta)$ (dashed line).

We notice first that, for small δ, the second kind FSLE curves tend to diverge as $\sim \delta^{-1}$ as can be predicted by simple arguments (Boffetta et al., 2000a). At small perturbation sizes (up to the mesoscale) the differences in the velocity fields are important and relative dispersion is not correctly estimated with the M and Y models or, in other words, the error in the trajectory evolution depends strongly on the differences between models. At gyre-scales (> 100) km, both $\lambda_{\mathrm{II}}^{(\mathrm{MD})}(\delta)$ and

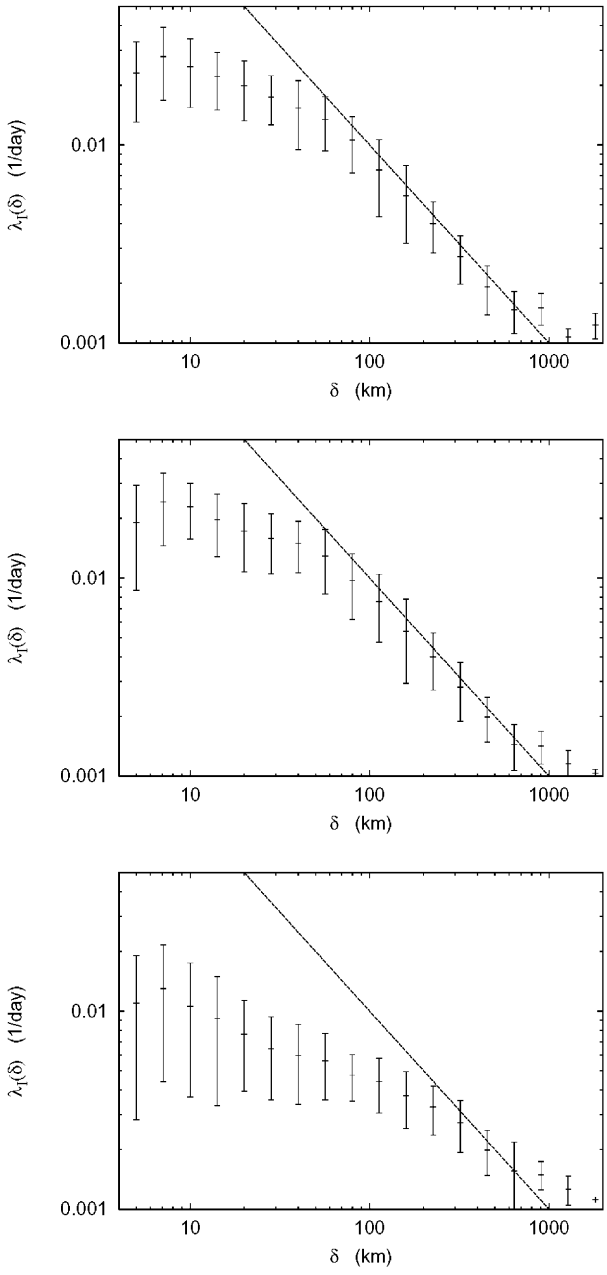

Fig. 3. First kind FSLE for particles advected with the D, M and Y in the upper, intermediate and lower panel, respectively, with $r = \sqrt{2}$.

$\lambda_{\mathrm{II}}^{(\mathrm{YD})}(\delta)$ converge to $\lambda_{\mathrm{I}}^{(\mathrm{D})}(\delta)$, indicating that, in this range, the model differences are not relevant to Lagrangian dynamics, and that dispersion rates on these scales can be estimated also with coarse sampling models.

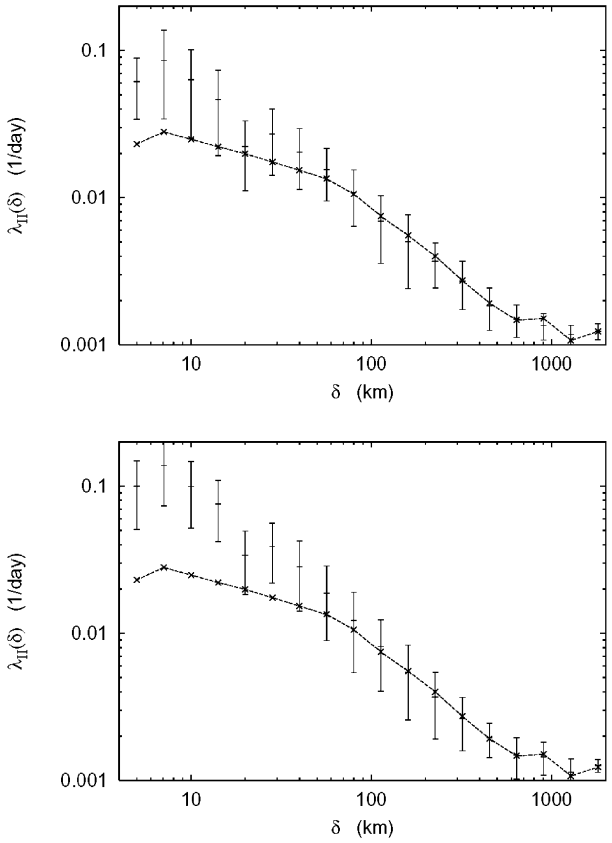

Fig. 4. Second kind FSLE for the M and D models (upper panel) and for the Y and D models (lower panel). The dashed line represents the mean value of $\lambda_1^{(D)}(\delta)$ with $r = \sqrt{2}$.

5. Spatial distribution of the second kind FSLE

In the oceans, Lagrangian variability is determined both by the spatial dishomogeneities and by the time variability of the Eulerian velocity field even if in some particular region one of the two limiting cases of *frozen turbulence* (prevalence of spatial dishomogeneities over time variability of the Eulerian velocity field) and of *fixed drifter* (prevalence of time variability over spatial dishomogeneities) can prevail (Figueroa and Olson, 1994; Lumkpin et al., 2002). In the frozen turbulence field approximation, the Eulerian field evolves slowly if compared to the advective time and Lagrangian velocity decorrelates because the particle samples regions that are spatially decorrelated. On the other hand, in the fixed drifter regime, the Lagrangian particles move slowly in the Eulerian field and before particles start exploring regions that are spatially decorrelated the time variability of the Eulerian field has already affected the partice motion. It may be then worth to visualize the regions of higher Lagrangian unpredictability due to the time sampling of the velocity field and to relate the observed geographical variability to known properties of the surface circulation field. Here we perform a preliminary analysis and in a forthcoming paper, we

will analyse in more detail relations between Lagrangian unpredictability and more classical kinematical and statistical quantities as, for example, EKE and ratio between Eulerian and Lagrangian correlation times.

We compute (2-D) second kind FSLE maps, defined as the spatial distribution of $\lambda_{\mathrm{II}}^{(\mathrm{MD})}(\delta)$ and $\lambda_{\mathrm{II}}^{(\mathrm{YD})}(\delta)$ over the initial positions. The computation starts when the distance between trajectories is $\delta = 5$ km and stops when a maximal distance is reached, $\delta = 50$ and 500 km (equivalent to setting $r = 10$ and $r = 100$, respectively). In Fig. 5 ($r = 10$ case), a general increasing of Lagrangian unpredictability is observed when passing from the MD to the YD map, due to the monthly mean variability of the velocity field.

Lagrangian unpredictability displays maximal values along the North African coast and low values in the Tyrrhenian, in the Adriatic and in the northern Ionian Seas. In particular, the highest values of λ_{II} are observed in correspondence of the Algerian Current, in the western basin,

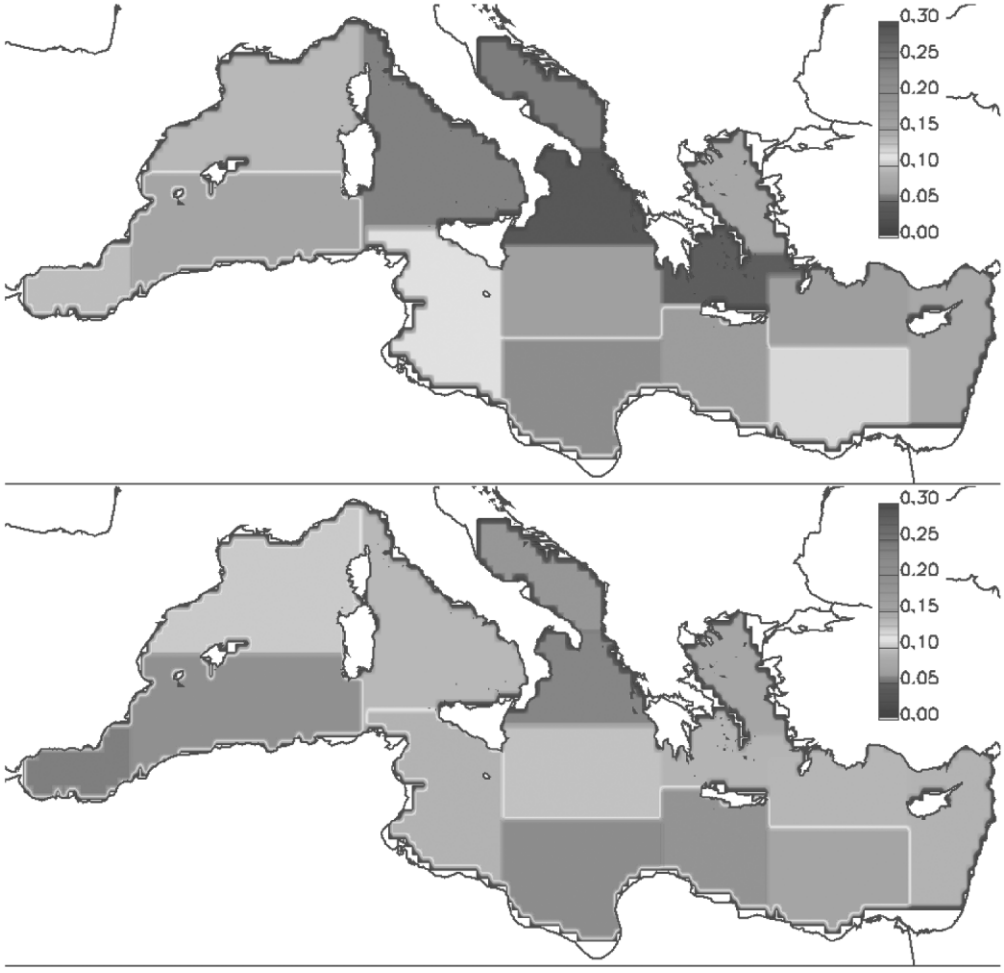

Fig. 5. Second kind FSLE map for the MD (upper panel) and YD case (lower panel), $r = 10$.

(see Fig. 1). This current flows close to the African coast in the western part of the basin, it is known to be one of the most intense surface currents of the Mediterranean Sea; horizontal shears are $\sim 10^{-5}$ s^{-1} and it is characterized by the recurrence of large anticyclonic eddies (Millot, 1999), due to baroclinic current instability. Another maximum is in correspondence of the Mid-Mediterranean Jet (MMJ), in Levantine basin (see Fig. 1), a baroclinic jet characterized by large meanders. Therefore, in both the previously mentioned regions, high values for λ_{II} are due to time variability of intense shear currents and Lagrangian time scales, in such cases, are due to intrinsic chaotic properties and not to the Eulerian time variability (frozen turbulence). The high values in the southern Ionian Sea has a different explanation because the circulation is not energetic as in the other two areas while time variability of the Eulerian fields, due to wind forcing, plays a major role (fixed drifter scenario). A comparison with estimates of Eulerian time scales, EKE and horizontal diffusivity from altimetric and in situ data confirmed this conclusion (Iudicone et al.,

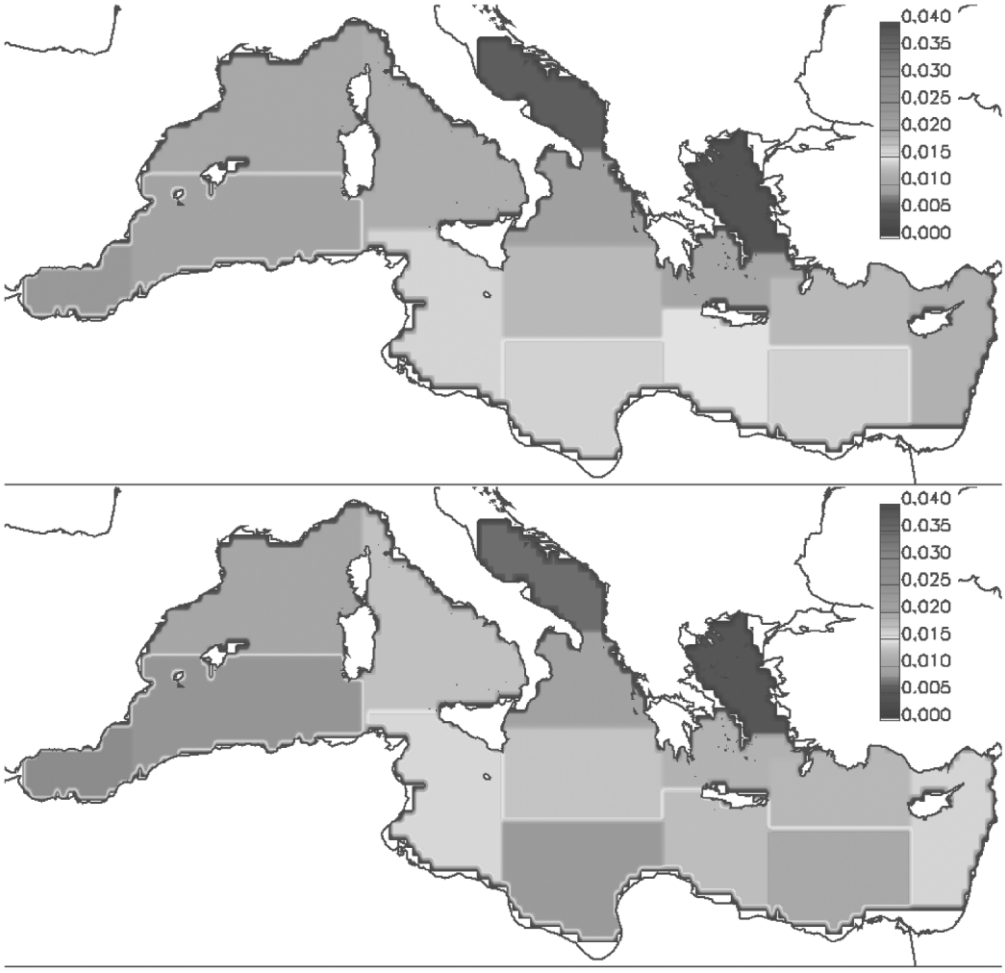

Fig. 6. Second kind FSLE map for the MD (upper panel) and YD case (lower panel), $r = 100$.

2001; manuscript in preparation). In the YD case, the large values of FSLE extend to the Alboran sea and evidence the role of the Atlantic Jet instabilities. It is interesting to observe that, in the Gulf of Lions region (North Western Mediterranean), characterized by the presence of a large gyre, relatively high values of λ_{II} are reached only in the YD case as if the persistence of a large structure filters out forcing periods up to one month.

The overall structure obtained computing λ_{II} for the $r = 100$ case (Fig. 6) is similar, with maxima in the southern part of the basin; the difference between the two cases MD and YD is largely decreased but there are still some sampling sensitive regions, as for instance the Algerian Basin and the south-eastern basin. Absolute maxima are stronger in YD but the background value is similar.

6. Discussion

Recently Samelson (1992) and Yang and Liu (1997) pointed out that modeled ocean circulation can be chaotic even when dealing with its steady (for 3-D models) or slowly varying component. Classic diffusion theory is not valid when asymptotic conditions are not fulfilled, i.e., on finite scales where advection overwhelms small-scale turbulent motions and long-term correlations persist. A number of shortcomings encountered with standard one-particle statistics are highlighted in e.g., Figueroa and Olson (1994), such as the non-convergence of the local diffusivity and the consequent rejection of a large amount of statistics. We used a dynamical system approach to characterize Lagrangian two-particle dispersion in non-asymptotic conditions via the FSLE technique. In this way, we have a tool to measure dispersion rates at any scale, independently from the assumption of small-scale turbulence as a model of tracer dispersion. This method allows to study and measure relative dispersion in a bounded flow as in the Mediterranean Sea and to clarify the effects of uncertainties on the velocity field, in our case due to different smoothing times, upon Lagrangian predictability. The presence of shear dispersion ($\lambda_I(\delta) \sim \delta^{-1}$) has been observed over scales $\sim$200–300 km, likely due to the persistence of a non-zero mean relative velocity between particles moving along separated current systems. On the other hand, at smaller scales, a plateau-like behavior ($\lambda_I(\delta) \sim$ constant) suggests the presence of chaotic advection. The effect of coarse time sampling is relevant at small and mesoscales < 100 km whereas at gyre and sub-basin scales > 100 km the differences between the velocity fields generate no more unpredictability than that intrinsically observed in each of the single fields.

It has been shown, by means of 2-D maps of the second kind FSLE, that the regions in which dispersion properties are most sensitive to the space and time variability of the velocity field can be identified. The effects of chaotic advection are important, are related to local dynamical processes, and are cause of Lagrangian non-stationarity in the most energetic regions, like in the Algerian Basin, while in region with high time variability of the Eulerian field, Lagrangian predictability is determined also by other time scales (e.g., wind ones). It is to note that, as a consequence, being FSLE a direct measure of the Lagrangian predictability (i.e., dispersion), there is not a one-to-one correspondence with classical *oceanographic* quantities, like horizontal shears (e.g., from altimetry) or current variability (e.g., from moorings), a part from situations *local* in space and, sometimes, in time.

We focused on off-line Lagrangian diagnostics and on the Mediterranean Sea circulation but some conclusions can be generalized. In fact, in ocean modeling the reliability in the occurrence of one of the two dispersion scenarios here discussed is largely influenced by, respectively, the model spatial resolution (e.g. shears) and choice of the forcings data sets (e.g. when dealing with monthly forcings climatologies). In a comparison with drifters data, for instance, we have found that the first kind FSLE of the real Algerian Current are in qualitative agreement with our modelling estimates (e.g., predominance of shear effects) but the absolute values are underestimated (by roughly a factor 2–5) because of unresolved shear spatial scales (Iudicone et al., 2001; manuscript in preparation).

Acknowledgements

We are deeply grateful to V. Artale and B. Blanke for their support respectively in the Eulerian and Lagrangian computations. We thank also G. Boffetta, A. Celani and M. Cencini for helpful discussions on the problem of the second-kind predictability, and E. Böhm, F. Bignami and S. Rossetto for a critical reading of this manuscript. This work was funded by the TRACMASS project (UE contract no. MAS3-CT97-0142 MAST III).

References

Artale, V., Boffetta, G., Celani, A., Cencini, M., Vulpiani, A., 1997. Dispersion of passive tracers in closed basins: beyond the diffusion coefficient. Physics of Fluids 9, 3162.

Artale, V., Iudicone, D., Santoleri, R., Rupolo, V., Marullo, S., D'Ortenzio, F., 2002. The role of surface fluxes in OGCM using satellite SST. Validation and sensitivity to forcing frequency of the Mediterranean thermohaline circulation. J. Geophys. Res. (in press).

Blanke, B., Arhan, M., Madec, M., Roche, S., 1999. Warm water paths in the equatorial atlantic as diagnosed with a general circulation model. Journal of Physical Oceanography 29, 2753.

Boffetta, G., Celani, A., Cencini, M., Lacorata, G., Vulpiani, A., 2000a. The predictability problem in systems with an uncertainty in the evolution law. Journal of Physics A 33, 1313.

Boffetta, G., Celani, A., Cencini, M., Lacorata, G., Vulpiani, A., 2000b. Non asymptotic properties of transport and mixing. Chaos 10 (1), 50.

Döös, K., 1995. Interocean exchange of water masses. Journal of Geophysical Research 100, 13499.

Figueroa, H.A., Olson, D.B., 1994. Eddy resolution versus eddy diffusion in a double gyre GCM. Part I: the Lagrangian and Eulerian description. Journal of Physical Oceanography 24, 371.

Haines, M.A., Fine, R.A., Luther, M.E., Ji, Z., 1999. Particle trajectories in an Indian ocean model and sensitivity to seasonal forcing. Journal of Physical Oceanography 29, 584.

Joseph, B., Swathi, P.S., 1999. Lagrangian particle transport in the Indian Ocean: a model study. Journal of Geophysical Research 104, 5211.

Lacasce, J., Bower, A., 2000. Relative dispersion in the subsurface Nort Atlantic. Journal of Marine Research 58, 863–894.

Lorenz, E.N., 1996. Predictability: a problem partly solved. In: Predictability, Proceedings of seminars held at ECMWF, (vol. 1), p. 1.

Lumkpin, R., Treguier, A.-M., Speer, K., 2002. Lagrangian eddy scales in the northern Atlantic Ocean, Journal of Physical Oceanography (in press).

Millot, C., 1999. Circulation in the western mediterranean. Journal of Marine System 99, 423.

Ottino, J.M., 1989. The Kinematics of Mixing: Stretching, Chaos and Transport. Cambridge University, Cambridge.

POEM Group, 1992. General circulation of the eastern mediterranean. Earth Science Reviews 32, 285.
Roussenov, V., Stanev, E., Artale, V., Pinardi, N., 1995. A seasonal model of the Mediterranean Sea. Journal of Geophysical Research 99, 13515.
Samelson, R.M., 1992. Fluid exchange across a meandering jet. Journal Physics Oceanography 22, 431.
Yang, H., Liu, Z., 1997. The three-dimensional chaotic transport and the great ocean barrier. Journal of Physical Oceanography 27, 1258.